Journal of Porphyrins and Phthalocyanines
J. Porphyrins Phthalocyanines 2014; **18**: 305–315
DOI: 10.1142/S1088424614500035

Published at http://www.worldscinet.com/jpp/

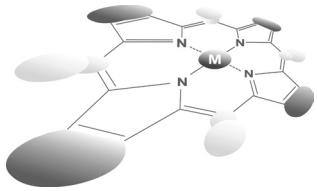

Optical, electrochemical, third-order nonlinear optical, and excited state dynamics studies of thio-zinc phthalocyanine

Debasis Swain[a], Varun K. Singh[b], Narra V. Krishna[b], L. Giribabu*[b] and S. Venugopal Rao*[a◊]

[a] *Advanced Centre of Research in High Energy Materials (ACRHEM), University of Hyderabad, Hyderabad 500046, India*
[b] *Inorganic and Physical Chemistry Division, Indian Institute of Chemical Technology, Hyderabad 500007, India*

Received 22 November 2013
Accepted 16 December 2013

ABSTRACT: Zinc phthalocyanine with S-aryl groups at α-positions have been synthesized and its optical, emission, electrochemical and third-order nonlinear optical properties were investigated. Both the Soret and Q-bands were red-shifted and obeyed Beer–Lambert's law. Electrochemical properties indicated that both oxidation and reduction processes were ring centered. Emission spectra were recorded in different solvents and the fluorescence yields obtained were in the range of 0.02 while time-resolved fluorescence data revealed lifetimes of typically few ns. Excited state dynamics in this novel thio-zinc phthalocyanine molecule has been investigated using femtosecond (fs) degenerate pump-probe spectroscopy. Nonlinear optical properties of this molecule have been examined using the Z-scan technique with picosecond (ps) and fs pulses. Both open and closed aperture Z-scan curves were recorded with ~2 ps/~150 fs laser pulses at a wavelength of 800 nm and nonlinear optical coefficients were extracted from both the studies. Degenerate pump-probe data performed at 600 nm suggested a single long lifetime of ~300 ps, possibly originating from the non-radiative decay of S_1 state.

KEYWORDS: femtosecond, pump-probe spectroscopy, Z-scan, phthalocyanine, fluorescence.

INTRODUCTION

Phthalocyanines are a versatile class of aromatic macrocycles with delocalized 18π-electron systems and possess extremely rich literature due to their unique optical, electronic, catalytic and structural properties [1–8]. The phthalocyanine (Pc) structure has been significantly scrutinized for improved chemical and physical properties and it is the elegant modification of Pc structure that has been demonstrated to effectively improve its photochemical and photophysical properties. Because of diverse redox chemistry, and high thermal/chemical stability, various applications such as semiconductors, electro-chromic displays, chemical sensors, sensitizers in solar cells, photodynamic therapy, and optical properties have motivated the researchers to synthesize various types of Pcs. Due to their planar π-conjugated system they are well suited for third-order nonlinear optical (NLO) response and possess exceptional stability against photoirradiation. The NLO property of metallophthalocyanines can be improved by changing the central metal atom, peripheral/axial position, and/or its aggregation state. Various research groups, including our group, have studied in detail the NLO response of a number of phthalocyanines with different central metals and peripheral substitutions [9–22]. The luminescence properties of Pcs are of interest because of their structural similarities to the porphyrins. The UV-vis absorption spectra of phthalocyanines demonstrated a Soret band of 360 nm and a Q-band at 684 nm without substitution at peripheral positions [23]. Typical fluorescence/

◊SPP full member in good standing

*Correspondence to: S. Venugopal Rao, svrsp@uohyd.ernet.in and soma_venu@yahoo.com, giribabu@iict.res.in

emission spectra of zinc phthalocyanines were also observed. Phthalocyanines are excellent singlet oxygen generators with a high value of quantum yield of singlet oxygen production of 0.59–0.80, as well as a fluorescence quantum yield production higher than that of porphyrins [24, 25]. It was demonstrated that the metallophthalocyanines exhibit stronger NLO responses than free-base phthalocyanines. A major disadvantage of phthalocyanines, however, is their low solubility in common organic solvents which further causes impediments for many practical applications. Therefore, one has to come up the design of phthalocyanines which render enhanced solubility and anticipated superior properties. The solubility of phthalocyanines in non-polar solvents can be improved by introducing different kinds of bulky groups like alkyl, alkoxy, alkylthio and crown ether groups on the phthalocyanine framework [26–28]. To fully explore the photosensitizing qualities of ZnPc, a detailed description of the intramolecular processes, occurring on time scales ranging from femtoseconds to microseconds, is required. Several experimental studies on the photo-physics of ZnPc and similar compounds (derivatives or different metallophthalocyanines) in solution have been reported, but so far the results fail to depict a coherent picture of the overall photo-physics [29, 30]. The large optical nonlinearities of phthalocyanines due to delocalized π electrons are envisaged in applications such as optical processing devices, practical optical limiters, and all-optical switches. Furthermore, new molecules with high two-photon absoprtion (2PA) and three-photon absorption (3PA) coefficients and cross-sections are interesting for their potential applications in photonics and biomedical applications [31]. Thiol substituted metallophthalocyanines show rich spectroscopic and photochemical properties as they absorb at longer wavelengths (>700 nm) than other metallophthalocyanines [32–35]. Various groups in the past have studied their photophysical and photochemical properties. However, their NLO properties have been limited in the literature. Herein, we report the synthesis of a phenyl thio phthalocyanine with eight *tert*-butylphenyl thio substituents at the non-peripheral positions. Their photophysical and photochemical studies along with their ultrafast NLO responses have been studied and the results are presented in this work.

EXPERIMENTAL

Materials

2,3-dicyanohydroquinone, trifluromethanesulphonic anhydride, 4-tertiarybutylbenzenethiol, 1-pentanol, 1,8-diazabicyclo[5.4.0] undec-7-ene(DBU) were purchased from Sigma Aldrich and were used as it is. All the solvents *viz*, dichloromethane, tetrahydrofuran, dimethylsulfoxide, *N*,*N*-dimethylformamide, toluene, methanol, potassium carbonate, chloroform, *n*-haxane were purchased from SD Fine chemicals Limited, India and were dried before further use. Zinc Acetate was purchased from Qualigens Chemicals Ltd, India.

Instrumentation

Absorption spectra were recorded with a Shimadzu UV-3600, by using 1×10^{-6} M solutions. Steady-state fluorescence spectra were recorded using a Fluorolog-3 spectrofluorometer (Spex model, Jobin Yvon) for solutions with optical density at the wavelength of excitation (λ_{ex}) ≈ 0.05. Fluorescence quantum yields (ϕ) were estimated by integrating the fluorescence bands of zinc *tert*-butyl phthalocyanine (ϕ = 0.37 in benzene) [36]. Fluorescence lifetime measurements were carried out using a ps time-correlated single photon counting (TCSPC) setup (FluoroLog3-Triple Illuminator, IBH Horiba Jobin Yvon) employing a ps light emitting diode laser (NanoLED, λ_{ex} = 670 nm) as excitation source. The decay curves were recorded by monitoring the fluorescence emission maxima of the phthalocyanine macrocycle (λ_{em} = 700 nm). Photomultiplier tube (R928P, Hamamatsu) was employed as the detector. The lamp profile was recorded by placing a scattered (dilute solution of Ludox in water) in place of the sample. The width of the instrument function was limited by full width at half maximum (FWHM) of the excitation source, ~635 ps at 670 nm. Decay curves were analyzed by nonlinear least-squares iteration procedure using IBH DAS6 (version 2.3) decay analysis software. The quality of the fits was judged by the X^2 values and distribution of the residuals.

Electrochemical measurements were performed on a PC-controlled CH instruments model CHI 620C electrochemical analyzer. The experiments were performed on 1 mM phthalocyanine solution in CH_2Cl_2 solvent at scan rate of 100 mV/s using 0.1 M tetrabutyl ammonium perchlorate (TBAP) as supporting electrolyte. The working electrode is glassy carbon, standard calomel electrode (SCE) is reference electrode and platinum wire is an auxiliary electrode. After a cyclic voltammogram (CV) had been recorded, ferrocene was added, and a second voltammogram was measured. The optical thin layer electrochemical studies were carried on Maya 2000 Ocean Optics software using DT-MINI-2-GS, UV-VIS-NIR LIGHTSOURCE. ^{1}H NMR spectra were recorded in $CDCl_3$ solutions on AVANCE 300 MHz spectrophotometer using TMS as standard. FT-IR spectra (KBr pellets) were recorded on a Perkin Elmer Spectrophotometer. Mass spectra were acquired using Electro Spray Ionization (ESI) method, operated in positive ion mode using *m/z* range 100–2000.

Synthesis

Synthesis of phthalonitrile-3,6-ditriflate (1). 2,3-dicyanohydroquinone (4.80 g, 30 mmol) in dichloromethane (100 mL) and pyridine (5.93 g, 75 mmol)

was treated with trifluoromethane sulphonic anhydride (21.16 g, 75 mmol) under nitrogen at −78 °C. After the reaction, mixture was allowed to cool to room temperature, stirring was continued for 24 h. The mixture was poured into water and the organic layer was extracted using dichloromethane. The extract was washed in turn with water, 2% hydrochloric acid, water, brine and water, and dried on sodium sulphate. The filtrate and the solvent evaporated and the crude product obtained was recrystallized from dichloromethane to afford the desired compound as colorless solid. ^{1}H NMR (500 MHz; $CDCl_3$; Me_4Si): δ, ppm 7.99 (s, 2H). FT IR (KBr): ν, cm^{-1} 3114 (ν_{C-H}), 2254 (ν_{C-N}), 1602 (ν_{C-H}), 1474 (ν_{C-H}), 1133 ($\nu_{S=O}$).

Synthesis of 3,6-bis(4-*tert*-butylthiophenyl)phthalonitrile (2). In a mixture of **1** (0.85 g, 2 mmol), potassium carbonate (1.16 g) and dimethyl sulphoxide (15 mL), 4-*tert*-butylthiophenol (4 mmol) was added, the mixture was reacted at room temperature for 24 h in nitrogen atmosphere. The reaction products were poured into water and the organic layer extracted using dichloromethane, and dried on sodium sulphate. The filtrate and the solvent evaporated and the crude product obtained was washed with methanol and recrystallized from toluene to obtain pure compound as yellow solid. ^{1}H NMR (300 MHz; DMSO-d_6; Me_4Si): δ, ppm 7.46–7.39 (m, 8H), 7.0 (s, 2H), 1.31 (s, 12H). FT IR (KBr): ν, cm^{-1} 3058 (ν_{C-H}), 2958 (ν_{C-H}), 2215 (ν_{C-N}), 1667 (ν_{C-C}), 1530 (ν_{C-C}), 1482 (ν_{C-C}), 1262, 830 (ν_{C-C}).

Synthesis of 1,4,8,11,15,18,22,25-octakis(4-*tert*-butylthiophenyl)Zn(II) phthalocyanine (Thio-Zn-Pc). A 50 mL round bottom flask was charged with **2**, $Zn(OAc)_2$ in dry 1-pentanol and heated at 100 °C. To this catalyst, 1,8-diazabicyclo[5.4.0] undec-7-ene (DBU) was added and the resultant solution was heated at 140 °C for 16 h and then cooled to room temperature. Pentanol was then removed under high vaccum and the solid green material was precipitated from methanol which was then subjected to silica gel column chromatography and eluted with hexane-chloroform to chloroform methanol. The brown phthalocyanine compound obtained was reprecipitated from methanol to afford the pure compound. Elemental analysis of anal. calcd. for $C_{112}H_{112}N_8S_8Zn$% (1892.05): C, 71.10; H, 5.97; N, 5.92. Found C, 71.15; H, 5.93; N, 5.96. UV-vis (DCM): λ_{max}, nm 803, 717, 511, and 358. MALDI-TOF: *m/z* ($C_{112}H_{112}N_8S_8Zn$) 1888 (calcd. for $[M]^+$).

NLO experimental details

Thio-Zn-Pc was synthesized according to the procedures reported in the literature [37] and were purified before use. The details of molecular structure and the absorption spectra have been reported elsewhere [38]. All the experiments were performed with samples dissolved in tetrahydrofuran (THF) and placed in 1-mm quartz cuvettes. Fs laser pulses were obtained from an oscillator (Chameleon, Coherent Inc.) delivering ~150 fs pulses at a repetition rate of ~80 MHz and centered at a wavelength of 800 nm. A regenerative amplifier (Legend, Coherent Inc.) provided 1 kHz pulses of ~2 ps duration, with a maximum output energy of ~2.0 mJ. The laser source was Ti:sapphire laser system (femtosecond LEGEND, Coherent) delivering nearly transform-limited pulses. The pulse duration was determined by external autocorrelation technique, by using ~2 mm thick BBO crystal in non-collinear geometry. A 200 mm focal length lens was used to focus the beam and the sample is scanned along the laser beam direction (Z-axis). The initial diameter of the input beam was ~3 mm. Complete details of Z-scan [39] experiments were reported in our earlier works [40–47].

The fs Z-scan measurements were performed in the spectral range of 600 nm–820 nm. For the fs Z-scan experiments the source was a tunable oscillator (Chameleon, Coherent) delivering ~150 fs pulses. A quartz cuvette (1-mm thick) containing the sample solution was traversed in the focusing geometry enabled by an achromat lens of 100 mm focal length. The beam waist ($2\omega_0$) at focal plane was estimated to be ~40 μm [FW($1/e^2$)M] with a corresponding Rayleigh range (Z_R) of ~1.5 mm ensuring the validity of thin sample approximation. Typically <30 nJ energy pulses were used for the experiments. The sample was translated using a high resolution stage (least count 10 μm) and the transmitted light was collected using a lens and a power meter (Coherent) combination. An aperture was placed in front of the lens for closed aperture scans and total light was collected during open aperture scans. Several neutral density filters were used to cut down the input intensity before the sample and also the intensity reaching photodiode. The translation stage moved mechanically with a step size of 1 mm and corresponding transmittance was recorded with the power meter. The sample was dissolved in THF to achieve ~0.1 mM concentration corresponding to a linear transmittance of >70% transmittance in all cases. The degenerate pump-probe experiments were carried out at 600 nm with pump-probe power ratios ranging from 20–50. The probe diameter was <1 mm and was always within the pump diameter of ~3 mm. Complete details of the pump-probe experiments are detailed in our earlier works [46].

RESULTS AND DISCUSSION

Synthesis and characterization

The synthetic route of 1,4,8,11,15,18,22,25-octakis(4-*tert*-butylthiophenyl)Zn(II) phthalocyanine is shown in scheme 1. Preparation of the complex was performed by reacting the phthalonitrile with $Zn(OAc)_2$, DBU in 1-pentanol. 2,3-dicyanohydroquinone was first treated with triflic anhydride and pyridine in dichloromethane at −78 °C

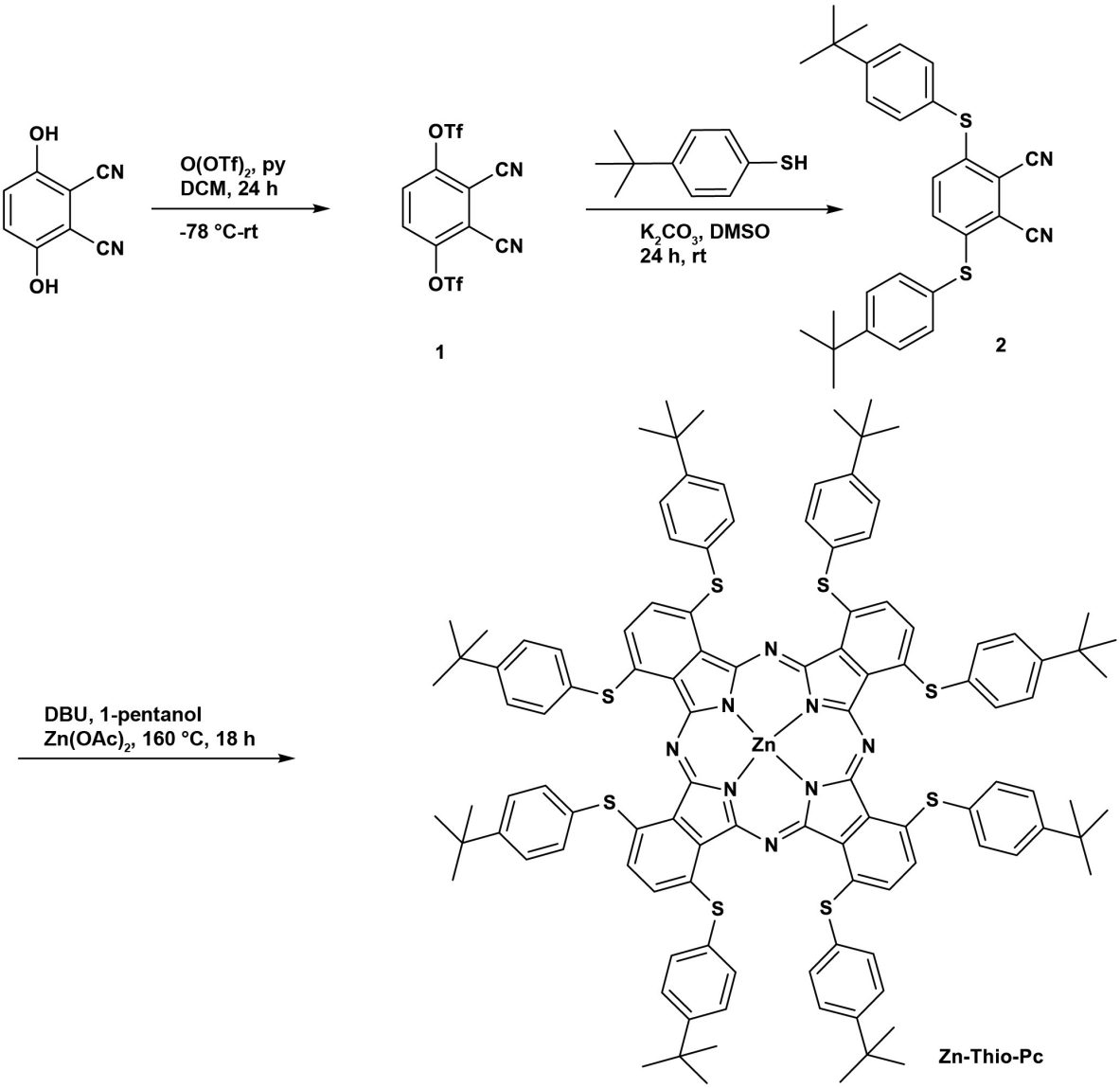

Scheme 1. Synthetic scheme of **Thio-Zn-Pc**

to get the 2,3-dicyanophenyl-bis(1,4-trifluoromethane-sulfonate) (**1**). The desired phthalonitrile, 3,6-bis(4-*tert*-butylphenylthio)benzene-1,2-dinitrile (**2**) was then obtained by reacting (**1**) with 4-*tert*-butyl benzenethiol in DMSO at room temperature. On cyclotetramerization of the phthalonitrile (**2**) in 1-pentanol at reflux temperature under the nitrogen atmosphere, the reaction mixture has turned to brown color. The brown colored cyclotetramerization complexe was purified by silica gel column chromatography, and was obtained in moderate yield. Preliminary characterization of **Thio-Zn-Pc** was done by using FT-IR and MALDI-MS. Cyclotetramerization of the compound can be seen clearly with the disappearance of the CN peaks at 2215 cm^{-1} in the FT-IR spectra of **Thio-Zn-Pc**. Methyl C–H peaks were also observed from 2900–3050 cm^{-1} for both the complexes. The mass spectra of **Thio-Zn-Pc** consisting of molecular ion peaks at *m*/*z* 1888 $[M]^+$ corresponds to the presence of molecule. Elemental analysis results were consistent with the assigned formulations.

UV-visible absorption studies

Typical phthalocyanine complex is known to exhibit two strong absorption bands arising from their orbital interactions and symmetry, one of them in the UV region near 300–400 nm arising from deeper π-levels to LUMO transition and the other in the visible part in the vicinity of 700 nm attributed to HOMO to LUMO transition (π–π*) of the Pc^{2-} ring. These intense band systems can be shifted or broadened depending on peripheral substitution, metallation and aggregation of the molecules. Substitution with strongly electron donating or strongly electron withdrawing groups potentially provide a method of

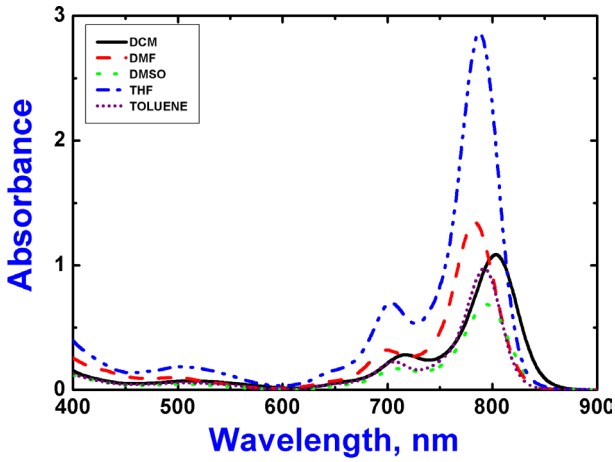

Fig. 1. Absorption spectrum of **Thio-Zn-Pc** in different solvents

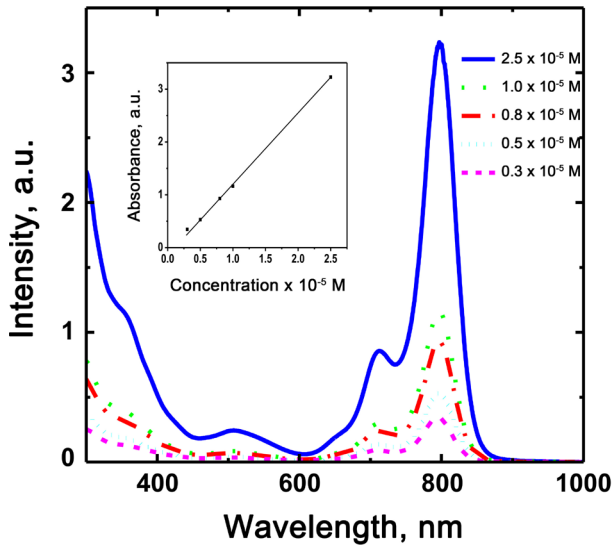

Fig. 2. Absorption spectral changes of **Thio-Zn-Pc** in DCM at different concentrations: (a) 0.3×10^{-5} (b) 0.5×10^{-5} (c) 0.8×10^{-5} (d) 1.0×10^{-5} (e) 2.5×10^{-5} M. Inset shows the plot of absorbance *vs.* concentration

tuning the Q-band absorption. The UV-vis spectrum of the **Thio-Zn-Pc** complex in various solvents, including DCM, is shown in Fig. 1. The complex exhibited a Q-band at around 796 nm and a B-band at 354 nm in the case of DCM. A new absorption peak was observed at 510 nm, a similar band appeared in thio substituted phthalocyanines reported in literature [48]. The spectra depicted monomeric behavior evidenced by a single narrow Q-band, typical of metallated phthalocyanine complexes [49]. The Q-band was considerably shifted to near IR region attributed mainly to the substitution of phthalocyanine ring at eight α-positions with arylthio substituents. The presence of suphur atoms further helps to red shift the absorption. The observed red spectral shift is typical of phthalocyanines with substituents at the non-peripheral positions [50, 51] and has been explained to be due to linear combinations of atomic orbitals (LCAO) coefficients at the non-peripheral positions of the HOMO being greater than those at the peripheral positions. As a result, the HOMO level is destabilized more at the non-peripheral position than it is at the peripheral position. Resultantly, the energy gap between the HOMO and the LUMO becomes smaller, consequently in a bathochromic shift.

Aggregates are undesirable not only for analytical purposes, for their absorbance spectra overlaps with that of the monomer, but also for practical device applications. The aggregation depends on concentration, solvent, substituents, complexed metal ions and temperature [52]. For many non-bulky or electron rich benzo substituted complexes, aggregation occurs readily, even at low concentrations, typically, used to record absorption spectra, making the spectral data more difficult to interpret. In dilute solutions phthalocyanines exist as single molecule and are surrounded by solvent molecules but with increasing concentration phthalocyanine molecules aggregate. In the aggregated state electronic structure of complex phthalocyanine rings are perturbed thereby altering the ground and excited state electronic structures [53]. Keeping this in mind, we have carried out the aggregation studies of **Thio-Zn-Pc** at different concentrations in DCM and the data is shown in Fig. 2. The complex clearly follows Beer–Lambert's law (Fig. 2 inset) for the monomeric species present in the solution as no aggregation tendency was observed evident from linear change of absorbance in the Q-band maxima.

Electrochemical studies

The phthalocyanine unit is a 18π-electron aromatic system that, in its common oxidation state, carries two negative charges. This unit is capable of oxidation, by losing one or two electrons, and reduction by gaining one to four electrons. The relative positions of the HOMO and LUMO levels can be shifted *via* changes in the electron density of the molecule brought about by electron donating or electron withdrawing substituents. To examine the redox properties of **Thio-Zn-Pc**, we have carried out electrolysis using the technique of cyclic voltammetry and differential pulse voltammetry. During reaction, four oxidation processes labeled I, II, III, IV (0.42. 0.76, 1.40 and 1.80 V *vs.* SCE) and two reduction processes labeled V and VI (−1.30 and −1.70 V SCE) were observed. Wave analysis suggested that, in general, first three oxidation steps are reversible (i_{pc}/i_{pa} = 0.9–1.0) and diffusion-controlled ($i_{pc}/\nu^{1/2}$ = constant in the scan rate (ν) range 50–500 mV/s) one-electron transfer (ΔE_p = 60–70 mV, ΔE_p = 65 ± 3 mV for ferrocenium/ferrocene couple) reactions, the subsequent steps are, in general, are quasi-reversible (E_{pa}–E_{pc} = 90–200 mV and i_{pc}/i_{pa} = 0.5–0.8 in the scan rate (ν) range 100–500 mV.s^{-1}).

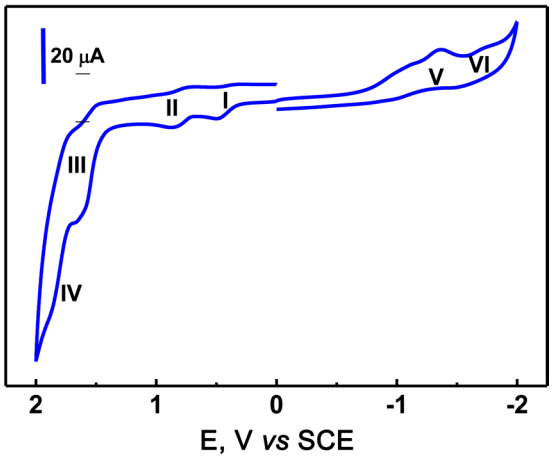

Fig. 3. Cyclic voltammogram of **Thio-Zn-Pc** in DCM at a glassy carbon electrode

The $E_{1/2}$ and $\Delta E_{1/2}$ values of complexes are in agreements with similar complexes in literature [54–60]. All the observed redox couples are ring based since the central metal is known to be electrochemically inactive for this complex [61]. Hence, the couple of peaks observed for **Thio-Zn-Pc** are associated with ring based processes.

Spectroelectrochemical measurements

Spectroelectrochemical studies were employed to confirm to monitor changes during redox reactions of **Thio-Zn-Pc**. Figures 4a–4g show the spectral changes of **Thio-Zn-Pc** during applied potential. During the controlled applied potential of 0.6 V, the intensity of the Q-band at 786 nm decreases without shift, while new bands at 523 and 932 nm region emerged. At the same time, the B-band at 387 nm decreases in intensity. The shoulder at 700 nm also decreases in intensity, which indicates disaggregation of the phthalocyanine macrocycle. During the process clear isosbestic points are observed at 342, 438, 659 and 833 nm, which clearly indicate that the oxidation gives a single product [62, 63]. Whereas, controlled oxidation potential at 1.0 V the Q-band decreased in intensity with a blue shift to 780 nm. The B-band decreased in intensity while an increase in intensity in the region 400 nm to 650 nm was observed. The new band formed at 932 nm during first oxidation also increased in intensity. On further controlled potential oxidations at 1.7 V and 2.0 V similar kind of changes were observed. During the controlled potential application at −1.2 V, blue shifting of the Q-band to 782 nm and observation of new band at 427 nm was observed and are assigned to be due to the ring based processes, $[Zn^{II}Pc^{-2}/Zn^{II}Pc^{-3}]^{-1}$. Then at the −1.6 V potential application, the intensity of the Q-band and band at 696 nm decreases in intensity with the formation of new bands at 467, 586 and 940 nm were recorded. The B-band present at 387 nm also decreases in intensity. The process shows clear isobestic points at 324, 431, 503, 637 and 832 nm. These spectroscopic changes are easily assigned to reduction of the monomeric species, $[Zn^{II}Pc^{-3}]^{1-}/[Zn^{II}Pc^{-4}]^{2-}$ dianionic species.

Emission properties

Qualitative evaluation of emission, including quantitative analysis of the fluorescence spectra and determination of the quantum yields (ϕ_f) was performed for **Thio-Zn-Pc** in order to understand the effect of peripheral substitution on phthalocyanine macrocycle. Figure 5 illustrates the emission spectra of

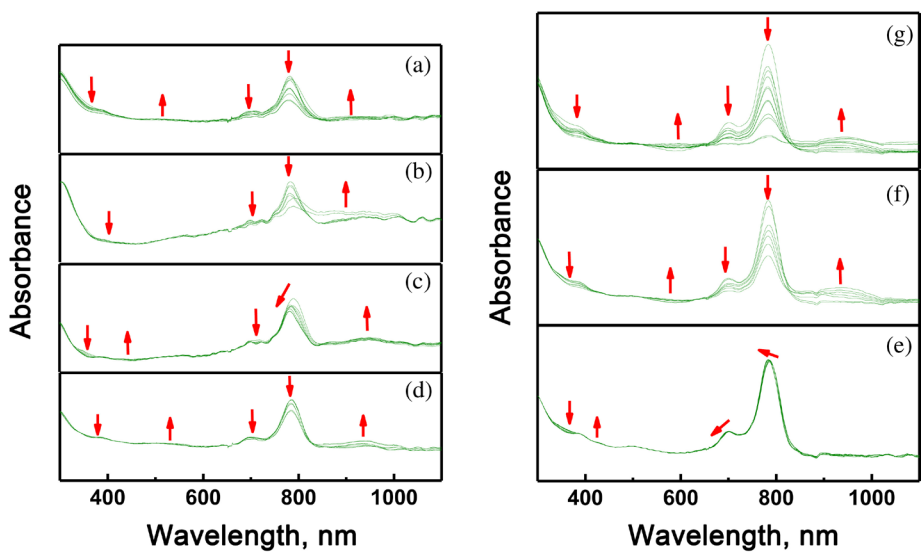

Fig. 4. *In situ* UV-vis spectral changes of **Thio-Zn-Pc** (a) E_{app} = 0.6 V (b) E_{app} = 1.0 V (c) E_{app} = 1.7 V (d) E_{app} = 2.0 V (e) E_{app} = −1.2 V (f) E_{app} = −1.6 V (g) E_{app} = −1.9V

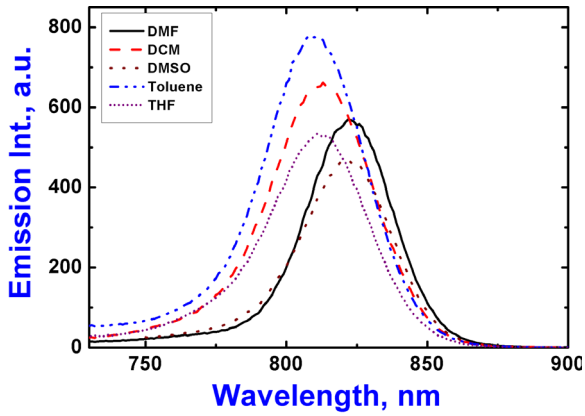

Fig. 5. Emission spectrum of **Thio-Zn-Pc** in different solvents

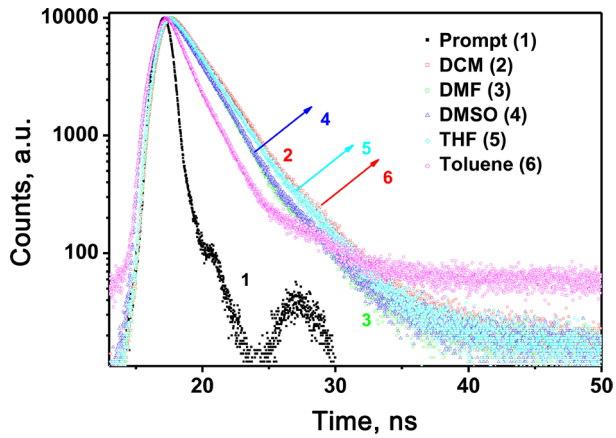

Fig. 6. Fluorescence decay signals of **Thio-Zn-Pc** in different solvents

Thio-Zn-Pc in toluene, DCM, THF, DMF and DMSO solvents by exciting phthalocyanine at 796 nm and the corresponding emission maxima and quantum yields are presented in Table 1. As it is apparent from data presented in Fig. 5 and Table 1 the emission spectra of **Thio-Zn-Pc** is consistent with both the Stokes rule and the rule of mirror symmetry between the absorption and fluorescence bands. From the data presented in Table 1, it is apparent that as the polarity of the solvent increases, the quantum yield reduced. This might be due to the increase of aggregation in polar solvents, which reduces the possibility of radiative deactivation *i.e.* fluorescence through dissipation of energy by the aggregates [64]. This in turn affects the singlet excited life time. Figure 6 displays the fluorescence decay signals of **Thio-Zn-Pc** in toluene, DCM, THF, DMF and DMSO solvents and the corresponding lifetime data presented is summarized in Table 1. We have observed biexponential decaly for all the solvents investigated in this study. The lifetimes presented in Table 1 is the majority component. Similar to the case of steady state emission, lifetimes were affected with polarity of the solvents used.

Nonlinear optical studies

Figures 7a and 7b illustrate the open aperture Z-scan data of **Thio-Zn-Pc** (~0.1 mM concentration) recorded at 800 with ~2 ps pulses nm (1 kHz repetition rate) and ~150 fs pulses (80 MHz repetition rate), respectively. Both the data depicted saturable absorption (SA), which is due to the presence of strong linear absorption at that particular wavelength. Closed aperture Z-scan data is presented in Figs 7c and 7d for ps and fs excitaitons, respectively. It is evident that in both the case the nonlinearity was negative. The magnitudes of n_2 were ~10^{-12} cm^2/W in fs (MHz repetition) case and ~10^{-16} cm^2/W in the ps (1 kHz repetition rate) case. The magnitudes of $\chi^{(3)}$ were large (~10^{-11} e.s.u.) in the fs case and moderate (~10^{-14} e.s.u.) in the ps case. Figures 8a–8f depicts the fs closed aperture data of Thio-Zn-Pc recorded at different wavelengths in the 700 nm–820 nm spectral range and the data clearly suggests negative nonlinearity with magnitudes of ~10^{-12} cm^2/W with a largest value of ~6.95×10^{-12} cm^2/W recorded at 760 nm. Figures 9a and 9b illustrate the typical open aperture data of **Thio-Zn-Pc** at 600 nm recored with ~2 ps pulses at lower (~60 GW/cm^2) and higher (~120 GW/cm^2) peak intensities, respectively. Interestingly, open aperture data at lower peak intensities depicted saturable absorption while the data at higher peak intensities depicted a switched behavior to reverse saturable absorption (RSA) with a two-photon absorption coefficient (β) of ~10^{-11} cm/W. In such type of molecules depending on the excitation wavelength and the input peak intensity SA or RSA or switching behavior (SA to RSA and vice-versa) prevails [10–16, 44–47]. For Z-scans performed away from resonance (strong linear absorption) we have observed switching mechanism from SA to RSA (see Supporting information) with both MHz, fs and kHz, ps excitation. The NLO coefficients extracted from the Z-scan studies are presented in Table 2 for both ps and fs excitation.

By appropriate tuning of the input wavelength, pulse duration, peak intensities with a fixed concentration of the molecules in solution one could obtain all the nonlinear absorption behaviours with these molecules. For example, with ns pulse excitation at 532 nm we could envisage RSA/ESA kind of behavior while with 800 nm ps/fs excitation

Table 1. Absorption, emission data of **Thio-Zn-Pc**

Sample	Solvent	λ_{max}, nm (log ε) $M^{-1}.cm^{-1}$	$\lambda_{em,\ max}$, nm	ϕ_f	τ_f, ns
Zn-Thio-Pc	DCM	803 (5.04)	823	0.020	1.23
	DMF	782 (5.13)	813	0.022	1.25
	DMSO	793 (4.84)	822	0.020	1.22
	THF	787 (5.45)	809	0.022	1.26
	Toluene	792 (4.99)	812	0.024	1.25

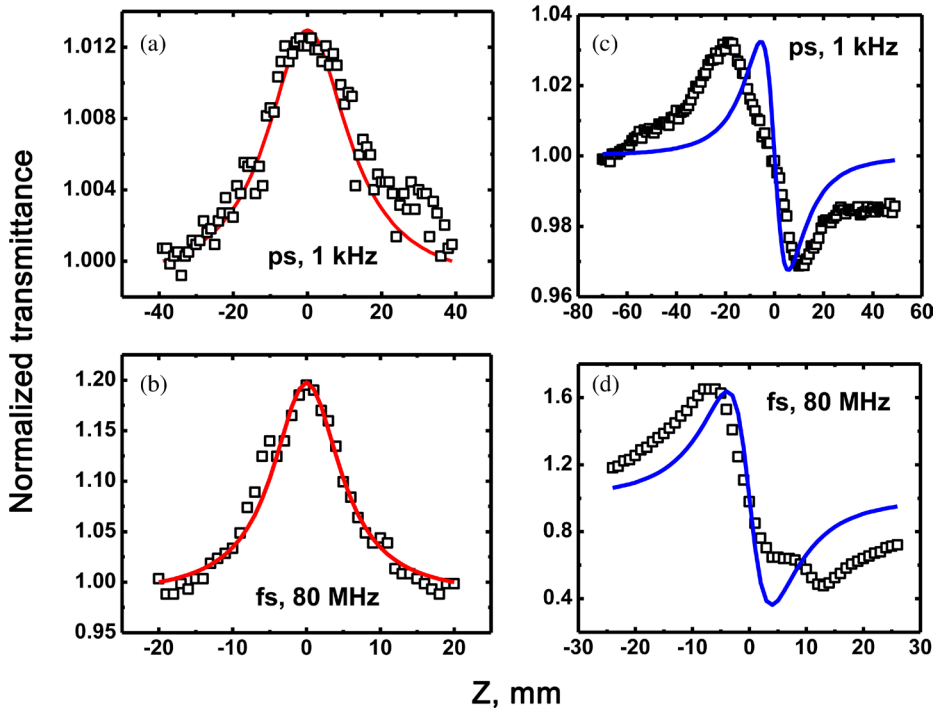

Fig. 7. OA behavior of **Thio-Zn-Pc** (in THF) at 800 nm depicting (a) SA with ~2 ps, 1 kHz excitation and (b) ~150 fs, 80 MHz excitaiton (**$I_s \ll I_{00}$**). Closed aperture data depicting negative nonlinearity in (c) ~2 ps, 1 kHz excitation (d) ~150 fs, 80 MHz excitation

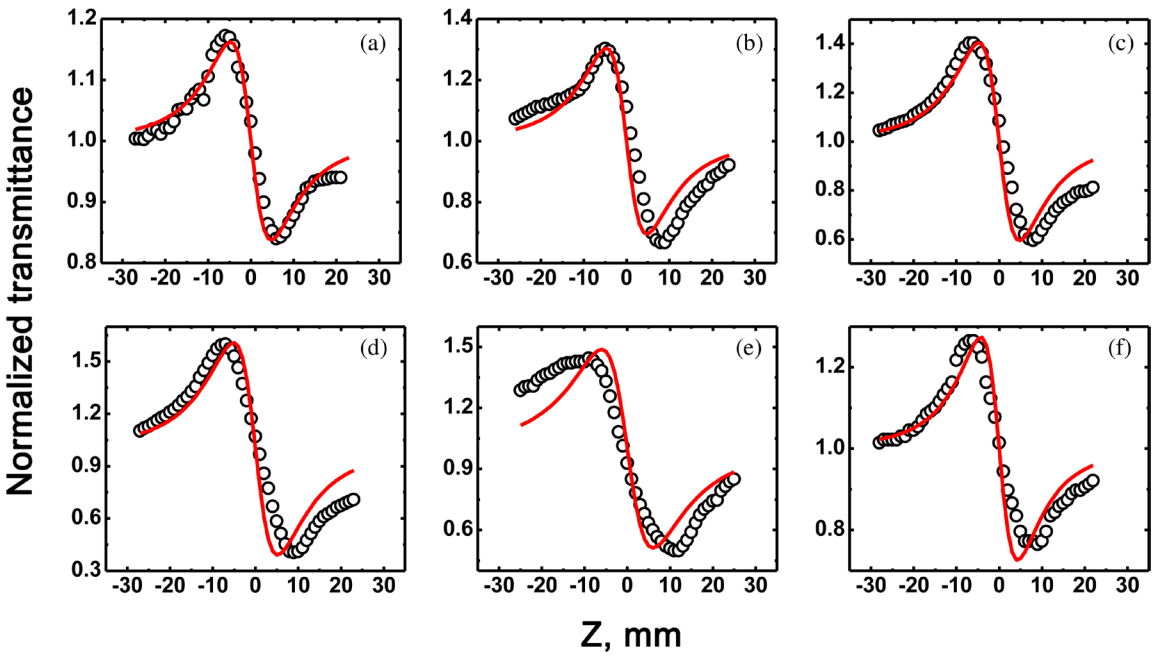

Fig. 8. Closed aperture data of **Thio-Zn-Pc** demonstrating negative nonlinearity at (a) 700 nm (b) 720 nm (c) 740 nm (d) 760 nm and (e) 780 nm and (f) 820 nm with 80 MHz, fs pulse excitation. n_2 values extracted from the fits were ~1.66×10^{-12} cm^2/W, ~2.10×10^{-12} cm^2/W, ~2.30×10^{-12} cm^2/W, ~6.95×10^{-12} cm^2/W, 4.36×10^{-12} cm^2/W and ~2.11×10^{-12} cm^2/W at respective wavelengths. The sign of n_2 was negative (self-defocusing)

we observed SA. For ps/fs excitaiton in the 600 nm–900 nm one can observe the switching mechanism of SA to RSA and with stronger and slective pumping one could achieve pure RSA (due to 2PA as was observed in the case at 600 nm). Though there are a number of reports on NLO studies of various phthalocyanines it is imperative that (a) a database of NLO properties of all novel phthalocyanines is created to facilitate establishing a structure-property

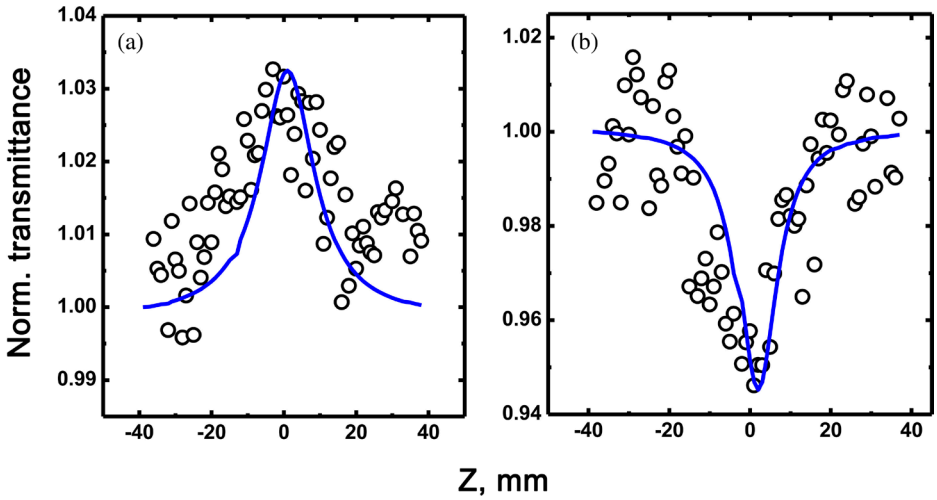

Fig. 9. (a) Open aperture Z-scan data of **Thio-Zn-Pc** at 600 nm with ~2 ps, 1 kHz excitation depicting (a) SA at 60 GW/cm^2 with $I_s > I_{00}$. I_s = 170 GW/cm^2 and (b) RSA at 120 GW/cm^2 with $\beta \sim 1 \times 10^{-11}$ cm/W. Solvent (THF) contribution was negligible in both cases

Table 2. Summary of NLO coefficients of **Thio-Zn-Pc** ($I_s < I_{00}$)

λ, nm	n_2, cm^2/W	I_s, W/cm^2	$\lvert Re[\chi^{(3)}]\rvert$	Total $[\chi^{(3)}]$
800 nm (~2 ps, 1 kHz)	-2.6×10^{-16}	5×10^{11}	1.3×10^{-14}	1.3×10^{-14}
800 nm (~150 fs, 80 MHz)	-9.3×10^{-13}	1×10^{7}	4.7×10^{-11}	4.7×10^{-11}

relationship [65–67] useful for synthesis of novel molecules and devices (b) nonlinearities are measured with short pulses (ps and fs) excitation in an attempt to identify the true electronic nonlinearities and their time response (c) congregate information on the spectral dependence of nonlinearities indispensable for identifying the spectral region of interest for various applications of n_2 and nonlinear absorption. Furthermore, NLO measurements with MHz pulses is also required since the repetition rates of lasers to be used in optical signal processing will be of similar magnitude to achieve high-speed data transmission rates (for example Gigabits/s to Terabits/s). It is well-understood and established that MHz repetition rate pulses induce thermal nonlinearities in open aperture Z-scan measurenents. However, one needs to discover mechanisms to identify the magnitudes of both electronic and thermal nonlinearities and separate them. One of the certain ways of reducing the thermal nonlinearities is to incorporate these molecules in media (*e.g.* polymers or glasses) possessing higher thermal diffusion coeffcients. Detailed investigations of dispersion studies (in the NIR spectral region) of NLO properties with both ps and fs pulses will be a subject of our future investigations.

Ultrafast pump-probe studies

Figure 10 depicts the degenerate pump-probe data of **Thio-Zn-Pc** recorded with ~70 fs pulses near 600 nm. It is evident from the data that ΔT/T was negative suggesting photo-induced absorption with a single exponential decay. The lifetime recovered from the fit to experimental data was a long one of ~309 ps. **Thio-Zn-Pc** is a radiative molecule with lifetimes of ~few ns. Therefore, the ~309 ps lifetime observed cannot be from the radiative transitions. Excitation with 600 nm pump photon could have excited the molecule to first excited singlet state due to small linear absorption at that wavelength. With strong pump inentisites (>100 GW/cm^2) two-photon absorption (2PA) is possible (see Supplementary material wherein the data is presented depicting 2PA in this molecule at 600 nm with stronger pumping and SA at weaker pumping). In the present case of pump-probe measurements the peak intensity of pump was much

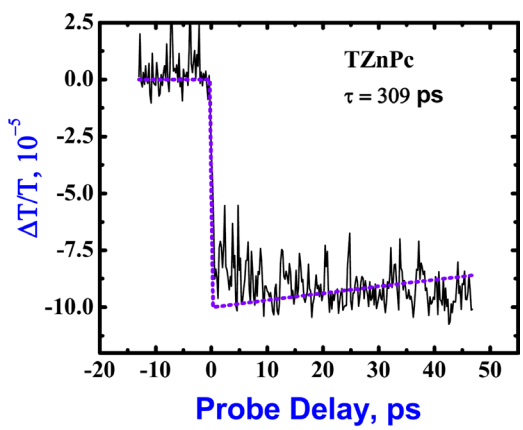

Fig. 10. Degenerate pump-probe data of **Thio-Zn-Pc** recorded with ~70 fs pulses at 600 nm. The fit depcits a single exponential decay of ~300 ps

lower than 120 GW/cm^2. Once excited into high lying states the molecules can come down to ground state *via* radiative and/or non-radiative mechanisms. The ~309 ps lifetime could be attributed to the non-radiaitve lifetime of S_1 states with possible contribution from inter-system crossing and/or radiative part. However, further detailed transient absorption studies are necessary to identify the exact contributions to this lifetime. Jarota *et al.* [68] have also investigated tetrasulfonated phthalocyanines (again similar molecules to ours) and observed lifetimes in the 150–500 ps range. They have assigned it to the S_1 to S_0 non-radiative decay mechanism. Howe *et al.* [69] investigated phthalocyanine and zinc phthalocyanine tetrasulfonate using ultrafast pump-probe spectroscopy slow life time of ~370 ps for the free base (PcS_4) and ~460 ps for the Zn substituted compound ($ZnPcS_4$). We had observed S_1 state lifetimes of <200 ps in similar organic molecules in some our earlier studies on porphycenes [46], corroles [70], and naphthobipyrroles [47]. Furthermore, in a few of our earlier works on phthalocyanines [71] and porphyrins [72, 73] we did observe sub-100 ps lifetimes (assigned to the S_1 state non-radiative decay) achived using incoherent laser spectroscopy. Fita *et al.* [74] observed <50 ps lifetimes for ester-alkyloxy substituted zinc phthalocyanines. They also observed ~ns lifetimes and assigned them due to the combination of inter-system crossing, radiative and non-radiative mechanisms. In our case the radiative lifetimes are >2 ns and, therefore, can safely assume miminal conrtibution from this.

CONCLUSION

In conclusion, we have explored photophysical, electrochemical, NLO properties of a thioaryl susbstituted zinc phthalocyanine. The absorption spectra was red-shifted due to non-peripheral substitution and obeyed Beer–Lambert's law. Spectroelectrochemical properties showed that the oxidation and redution processes were ring centered. NLO properties of Thio-Zn-Pc have been investigated using Z-scan technique with ps and fs pulses. Both open and closed aperture Z-scan curves were recorded with ~2 ps/~150 fs laser pulses at a wavelength of 800 nm and large nonlinear optical coefficients were extracted from both the studies. Excited state dynamics in this novel molecule investigated using fs degenerate pump-probe spectroscopy revealed a single exponential of ~300 ps, which has been assigned to the S_1 to S_0 state non-radiative lifetime.

Acknowledgements

S Venugopal Rao thanks the DRDO for continued financial support. LG thanks the CSIR-XII FYP '*Intel Coat*' project CSC-0114 and CSC-0134 ("Molecules to Materials and Devices M2D"). VKS and NVK thank the CSIR for research fellowships.

Supporting information

Figures S1–S8 are given in the supplementary material. This material is available free of charge *via* the Internet at http://www.worldscinet.com/jpp/jpp.shtml.

REFERENCES

1. Ragoussi ME, Ince M and Torres T. *Euro J. Org. Chem.* 2013; **2013**: 6475–6489.
2. Sorokin AB. *Chem. Rev*. 2013; **113**: 8152–8191.
3. Giribabu L, Kanaparthi RK and Velkannan V. *The Chem. Record* 2012; **12**: 306–328.
4. Wohrle D, Schnurpfeil G, Makarov SG, Kazarin A and Suvorova ON. *Macroheterocycles* 2012; **5**: 191–202.
5. Nyokong T. *Coord. Chem. Rev.* 2007; **251**: 1707–1722.
6. Nyokong TB. *Pure Appl. Chem.* 2011; **83**: 1763–1779.
7. Ishii K and Kobayashi N. In *The Porphyrin Handbook*, Vol. 16, Kadish KM, Smith KM and Guilard R. (Eds.) Academic Press/Elsevier: New York, 2003; Chapter 102, pp 1–40.
8. Dumoulin F, Durmuş M, Ahsen V and Nyokong T. *Coord. Chem. Rev.* 2010; **254**: 2792–2847.
9. Rao SV. *Proc. SPIE,* 2010; **7728**: 77281N.
10. Rao SV, Anusha PT, Giribabu L and Tewari SP. *Pramana — J. Phys.* 2010; **75**: 1017–1023.
11. Kumar RSS, Rao SV, Giribabu L and Rao DN. *Opt. Mat.* 2009; **31**: 1042–1047.
12. Rao SV, Giribabu L, Venkatram N and Rao DN. *J. Appl. Phys.* 2009; **105**: 053109.
13. Venkatram N, Giribabu L, Rao DN and Rao SV. *Appl. Phys. B.* 2008; **91**: 149–156.
14. Venkatram N, Giribabu L, Rao DN and Rao SV. *Chem. Phys. Lett.* 2008; **464**: 211–215.
15. Kumar RSS, Rao SV, Giribabu L and Rao DN. *Proc. SPIE* 2008; **6875**: 68751D.
16. Mathews SJ, Kumar CS, Giribabu L and Rao SV. *Mater. Lett.* 2007; **447**: 274–278.
17. Torre G, Vazquez P, Aqullo-Lopez F and Torres T. *J. Mater. Chem.* 1998; **8**: 1671–1683.
18. Maree MD, Nyokong T, Suhling K and Phillips D. *J. Porphyrins Phthalocyanines* 2002; **6**: 373–376.
19. Britton J, Durmuş M, Khene S, Chauke V and Nyokong T. *J. Porphyrins Phthalocyanines* 2013; **17**: 691–702.
20. Sanusi SO, Antunes E and Nyokong T. *J. Porphyrins Phthalocyanines* 2013; **17**: 920–927.
21. Henari F, Davey A, Blau W, Haisch P and Hanack M. *J. Porphyrins Phthalocyanines* 1999; **3**: 331–338.
22. Liu LC, Tai CH, Hu AT and Wei TH. *J. Porphyrins Phthalocyanines* 2004; **8**: 984–988.
23. Agar E, Samaz S, Akademir N and Keskin L. *Dalton Trans.*1997; **12**: 2087–2090.
24. Gurol I, Durmus M, Ashen V and Nyokong T. *Dalton Trans*. 2007; 3782–3791.

25. Owens JW, Smith R, Robinso R and Robins M. *Inorg. Chimica Acta* 1998; **279**: 226–231.
26. Fernández DA, Awruch J and Dicelio LE. *Photochem. Photobiol.* 1996; **63**: 784–792.
27. Ertem B, Bilgin A, Gok Y and Kanteki H. *Dyes Pigm.* 2008; **77**: 537–544.
28. Unlu S, Yarasir MN, Kandaz M, Koca A and Salih B. *Polyhedron* 2008; **27**: 2805–2810.
29. Bilgin A and Gok Y. *Supramol. Chem.* 2006; **18**: 491–499.
30. Rao SV and Rao DN. *Porphyrins Phthalocyanines* 2002; **6**: 233–237.
31. Savolainen J, Linden DVD, Dijkhuizen N and Herek JL. *J. Photochem. Photobiol.*, *A* 2008; **196**: 99–105.
32. García IAC, Sevim AM, de la Escosura A and Torres T. *Org. Biomol. Chem*. 2013; **11**: 2237–2240.
33. Sakamoto K, Ohno-Okumura E, Kato T and Soga H. *J. Porphyrins Phthalocyanines* 2010; **14**: 47–54.
34. Burnham PM, Cook MJ, Gerrard LA, Heeney MJ and Hughes DL. *Chem. Commun*. 2003; 2064–2065.
35. Cook MJ, Chambrier I, Cracknell SJ, Mayes DA and Russell DA. *Photochem. Photobiol*. 1995; **62**: 542–545.
36. Kumar RSS, Rao SV, Giribabu L and Rao DN. *Chem. Phys. Lett.* 2007; **447**: 274–278.
37. Lawrence DS and Whitten DG. *Photochem. Photobiol.* 1996; **64**: 923–935.
38. Singh VK, Salvatori P, Anna A, Saurabh A, Angelis FD, Nazeeruddin MK, Krishna NV and Giribabu L. *Inorg. Chim. Acta* 2013; **407**: 289–296.
39. Bahae MS, Said AA, Wei TH, Hagan DJ and Stryland EWV. *IEEE J. Quant. Electron.*1990; **26**: 760–769.
40. Anusha PT, Reeta PS, Giribabu L, Tewari SP and Rao SV. *Mater. Lett.* 2010; **64**: 1915–1917.
41. Saravanan KV, Raju KCJ, Krishna MG, Tewari SP and Rao SV. *Appl. Phys. Lett.* 2010; **96**: 232905–232907.
42. Podagatlapalli GK, Hamad S, Sreedhar S, Tewari SP and Rao SV. *Chem. Phys. Lett.* 2012; **530**: 93–97.
43. Rao SV. *J. Mod. Opt.* 2011; **58**: 1024–1029.
44. Sarma T, Panda PK, Anusha PT and Rao SV. *Org. Lett.* 2010; **13**: 188–191.
45. Rao SV, Prashant TS, Sarma T, Panda PK, Swain D and Tewari SP. *Chem. Phys. Lett.* 2011; **514**: 98–103.
46. Swain D, Anusha PT, Prashant TS, Tewari SP, Sarma T, Panda PK and Rao SV. *Appl. Phys. Lett.* 2012; **100**: 141109.
47. Swain D, Anusha PT, Sarma T, Panda PK and Rao SV. *Chem. Phys. Lett.* 2013; **580**: 73–77.
48. Ozturk C, Erdogmus A, Durmus M, Ugur AL, Kilicarslan FA and Erden I. *Spectrochimica Acta A* 2012; **86**: 423–431.
49. Stillman MJ and Nyokong T. In *Phthalocyanines: Properties and Applications*, Vol. 1, Leznoff CC and Lever ABP. (Eds.) VCH Publishers: New York, 1989; Chapter 3.
50. Anderso AB, Gorden TL and Kenney ME. *J. Am. Chem. Soc.* 1985; **107**: 192–195.
51. Konami M, Hatano M and Tajiri A. *Chem. Phys. Lett.* 1990; **166**: 605–608.
52. Enkelkamp H and Nolte RJM. *J. Porphyrins Phthalocyanines* 2000; **4**: 454–459.
53. Dominguez DD, Snow AW, Shirk JS and Pong RGS. *J. Porphyrins Phthalocyanines* 2001; **5**: 582–592.
54. Erdogmus A, Koca A, Ugur AL and Erden I. *Synthetic Metals* 2001; **161**: 1319–1329.
55. Lever ABP, Minor P and Wilshire JP. *Inorg. Chem.* 1981; **20**: 2550–2553.
56. Yaras MN, Kandaz M, Koca A and Salih B. *Polyhedron* 2007; **26**: 1139–1147.
57. Koca AI, Bayar S, Dinc HA and Gonca E. *Electrochimica Acta* 2009; **54**: 2684–2692.
58. Alemdar A, Özkaya AR and Bulut M. *Synthetic Metals* 2010; **160**: 1556–1573.
59. Akinbulu IA, Khene S and Nyokong T. *Electrochimica Acta* 2010; **55**: 7085–7093.
60. Matemadombo F, Maree MD, Ozoemena KI, Westbroek P and Nyokong T. *J. Porphyrins Phthalocyanines* 2005; **9**: 484–490.
61. Lever ABP, Milaeva ER and Speier G. In *Phthalocyanines: Properties and Applications*, Vol. 3, Leznoff CC and Lever ABP. (Eds.) VCH: New York, 1993; Chapter 1.
62. Stilman MJ. In *Phthalocyanines: Properties and Applications*, Vol. 3, Leznoff CC and Lever ABP. (Eds.) VCH Publishers: New York, 1993.
63. Stillman MJ and Thomson AJ. *J. Chem. Soc. Faraday Trans.* 1974; **70**: 790–804.
64. Ogunsipe A, Maree D and Nyokong T. *J. Mol. Struct.* 2003; **650**: 131–140.
65. de la Torre G, Vázquez P, Agulló-López F and Torres T. *Chem. Rev.* 2004; **104**: 3723–3750.
66. Hales JM, Barlow S, Kim H, Mukhopadhyay S, Brédas JL, Perry JW and Marder SR. *Chem. Mater.* In press 2013; dx.doi.org/10.1021/cm402893s.
67. Kuzyk MG, Singer KD and Stegeman GI. *Adv. Opt. Phot.* 2013; **5**: 4–82.
68. Jarota A, Tondusson M, Galle G, Freysz E and Abramczyk H. *J. Phys. Chem. A* 2012; **116**: 4000–4009.
69. Howe L and Zhang JZ. *J. Phys. Chem. A* 1997; **101**: 3207–3213.
70. Anusha PT, Swain D, Hamad S, Giribabu L, Prashant TS, Tewari SP and Rao SV. *J. Phys. Chem. C* 2012; **116**: 17828–17837.
71. Rao SV and Rao DN. *J. Porphyrins Phthalocyanines* 2002; **6**: 233–237.
72. Rao DN, Rao SV, Aranda FJ, Rao DVGLN, Nakashima M and Akkara JA. *J. Opt. Soc. Am. B* 1997; **14**: 2710–2715.
73. Rao SV, Naga Srinivas NKM, Rao DN, Giribabu L, Maiya BG, Philip R and Kumar GR. *Opt. Commun.* 2001; **192**: 123–133.
74. Fita P, Osmalek T, Goslinski T, Wierzchowski M and Mielcarek J. *J. Photochem. Photobiol. A. Chem.* 2012; **232**: 44–49.

